Vision Res. Vol. 28, No. 1, pp. 9–24, 1988
Printed in Great Britain.

0042-6989/88 $3.00 + 0.00

GAP JUNCTIONS IN THE INNER PLEXIFORM LAYER OF THE GOLDFISH RETINA

ROBERT E. MARC, WEI-LEY S. LIU and JAY F. MULLER

University of Texas Graduate School of Biomedical Sciences, Sensory Sciences Center, 6420 Lamar Fleming, Houston, TX 77030, U.S.A.

(*Received* 5 *July* 1986; *in revised form* 13 *July* 1987)

Abstract—Oblique thin sections of the goldfish inner plexiform layer (IPL) were examined to characterize the processes engaging in gap junctions. Omission of *en bloc* uranyl acetate staining enhanced the relative visibility of gap junctions, thus facilitating surveys. Three general categories were identified: (1) extensive gap junctions between large caliber amacrine cell dendrites presynaptic to ganglion cells and other amacrine cells in distal and proximal IPL; (2) moderate to small gap junctions between amacrine cell synaptic terminals or small amacrine cell-like processes of similar cytoplasmic appearance; and (3) gap junctions between the telodendria/terminals of bipolar cells. Most instances of gap junctions in the goldfish IPL seem to represent cases of homologous coupling. We have not found unambiguous cases of heterologous coupling as in the mammalian retina, nor have we yet found mixed synapses. Taken together with previous physiological and anatomical findings, homologous coupling occurs between pairs of rods, cones, horizontal cells, bipolar cells and amacrine cells in the goldfish retina, and this in turn implies that direct intercellular communication among like cell types is a common theme in retinal circuitry.

Retina Gap junctions Amacrine cells Bipolar cells

INTRODUCTION

Ultrastructural and electrophysiological evidence has indicated the presence of low resistance paths for ionic or molecular flow between certain eukaryotic cells. The phenomenon is commonly called intercellular coupling and its physical substrate is the gap junction (Lowenstein, 1975). The best studied cases of intercellular coupling in the retina involve gap junctions between pairs of photoreceptors and those between pairs of horizontal cells. Coupling is also present in the inner plexiform layer (IPL) as evidenced by gap junctions between type AII amacrine cells and certain cone bipolar cells in the cat retina (Famiglietti and Kolb, 1975). This is the definitive example of heterologous coupling, i.e. coupling between different kinds of cells. Type AII amacrine cells also appear to form gap junctions among themselves (Famiglietti and Kolb, 1975), which represents homologous coupling. Gap junctions have been observed in the IPLs of several mammalian species (Raviola and Raviola, 1967, 1982; Dowling, 1979), and have been attributed to several neurochemically or structurally identified varieties of amacrine cells (Famiglietti and Kolb, 1975; Kolb and Nelson, 1985; Marc and Liu, 1985). Corresponding anatomical examples in non-mammalian retinas have been infrequent. Four different teleost species have been shown to possess coupling among neurons in the IPL. Direct electrophysiological evidence and electron microscopy of catfish retinal neurons injected with horseradish peroxidase (HRP) demonstrated that catfish transient amacrine cells are coupled in a homologous network (Naka and Christensen, 1981). Homologous dye coupling has been detected among small clusters of transient amacrine cells and also among clusters of sustained On amacrine cells in carp retina (Teranishi *et al.*, 1984). Gap junctions have been observed between processes deriving from interstitial amacrine cells in the retina of *Astronotus ocellatus* (Zimmerman, 1983). Finally, there is electrophysiological evidence of homologous coupling between pairs of carp bipolar cells (Kujiraoka and Saito, 1986) and gap junctions have been observed between the synaptic terminals of bipolar cells in the cone-rich retina of the marine fish, *Callionymus lyra* (Van Haesendonck and Missotten, 1983b). The goldfish is closely related to the carp and has been a major model of retinal information processing, and we felt it appropriate to survey the goldfish IPL for the kinds of gap junctions observed in other teleost species.

Our conclusions are that gap junctions may

be found at any level of the goldfish IPL, that their apparent infrequency derived from infrequent systematic searches, sub-optimal staining tactics, sampling biases intrinsic to vertical sections, and possible non-uniform distributions of gap junctions. We further note that gap junctions occur between pairs of (1) large, smooth, microtubule-rich amacrine cell processes that may arise from transient amacrine cells, (2) medium-to-small amacrine cell terminals or processes, and (3) telodendria from bipolar cell terminals. Nearly all the instances we present may be classified as cases of homologous coupling. We have not yet observed any mixed synapses, i.e. a combination of a gap junction and a chemical synapse between a pair of profiles (e.g. Korte and Rosenbluth, 1980), nor gap junctions between identifiably dissimilar cell types.

METHODS

Fixation and staining

Retinas were isolated from the eyecups of light-adapted goldfishes killed by rapid cervical transection and pithing, fixed in mixed aldehydes, osmicated, dehydrated and embedded in epoxy resins as previously described (Marc *et al.*, 1978). A direct comparison was made between retinas that were or were not stained *en bloc* with uranyl acetate. Such retinas will be referred to as + EBUA and − EBUA preparations, respectively. *En bloc* staining was performed after osmication and before dehydration by rinsing the tissue in maleate buffer (0.1 M, pH 5.1, three rinses, 5 min each), immersing for 1 hr in 1% uranyl acetate in maleate buffer (0.1 M, pH 6.0), followed by another triple rinse in pH 5.1 maleate buffer. The rationale for the comparison is two-fold (see Hayat, 1981): (1) avoiding *en bloc* uranyl acetate staining preserves cytoplasmic differentiation and cell specific differences in glycogen content; (2) *en bloc* uranyl acetate staining renders almost all unit membranes of uniform electron density, whereas avoiding it preserves some differences between junctional and nonjunctional unit membranes.

Sectioning

Oblique serial thin sections were cut with silver-gold to gold interference color and mounted on Formvar-filmed copper slot grids, stained with lead citrate and uranyl acetate, carbon coated and observed at 80 kV in a JEOL JEM 100-B electron microscope using either high contrast ACW or standard specimen carriers. ACW specimen carriers limit resolution but increase contrast, thus improving the visibility of gap junctions at low magnifications. The primary reason for using shallow oblique sections is that they increase the probability of encountering gap junctions. If gap junctions are randomly distributed through the IPL, the improvement in encounter frequency is simply the ratio of the volumes of IPL sampled in strict vertical vs oblique sections. By sectioning at an angle of approximately 20 deg from the horizontal plane of the IPL (0 deg), the volume of IPL sampled is three times that of a section of the same height, width and thickness taken vertically through the retina (90 deg from the plane of the IPL). There is abundant evidence, however, that many different kinds of dendrites, axons and synaptic terminals in the IPL are highly stratified (confined to narrow bands within the IPL) and patterned in mosaic-like arrays (Van Haesendonck and Missotten, 1983a, b; Marc, 1986). It is thus possible that a given population of gap junctions is constrained to a certain narrow band of the IPL and is regularly distributed within that level. If this were so, one would have to take into account the average size, spacing and degree of stratification of the gap junctions to determine the extent to which oblique sections improved encounter frequencies. We produced model systems to sample the encounter rate of section planes passing vertically or obliquely through variably sized strata containing variably spaced and sized targets. For targets of 1 μm diameter, constrained to a 1 μm thick plane, spaced in a square array 15 μm apart, 20 deg sections show five times the encounter frequency over vertical sections. From empirical observations, the ratio is at least this large. Sampling vertical sections did not turn out to be practical, however, because we failed to find any gap junctions in many vertical sections despite extensive examination. While this result was expected, it was very time consuming and unrewarding to carefully screen a vertical section only to conclude that we could not identify a gap junction. Most of our sections were taken at less than 20 deg but greater than 0 deg since truly horizontal sections result in a loss of orientation landmarks with a consequent inability to estimate the sublayer of the IPL in which gap junctions were encountered.

Identification of gap junctions

To establish the correspondence between the junctional arrangements observed in − EBUA preparations and those identified as gap junctions in + EBUA preparations, we performed scanning microphotometry on electron micrograph negatives and compared the superpositions of membrane leaflets. Negatives were scanned in a traverse perpendicular to the plane of the membrane in 10 or 20 μm steps with slits 5 or 10 μm wide, respectively, and 100 μm long (slit length parallel to the plane of the membrane). The different step sizes depended on the magnification of the negative. The slit dimensions were chosen to provide optical averaging in the plane of the scanned membrane and to prevent aliasing. All scans were scaled by dividing the absolute scan traverse in μm by the magnification of the negative.

Terminology

Certain words or expressions will be employed that require definition. *Distal* will indicate that, with respect to a reference element, a structure is closer to the photoreceptor layer than it is to the ganglion cell layer; *proximal* will indicate the converse. Thus the IPL is distal to the ganglion cell layer but proximal to the inner nuclear layer. The inner plexiform layer is a multilayered zone and will be divided into five arbitrary sublayers of equal thickness numbered in distal to proximal sequence as *sublayer 1* through *sublayer 5*. The face of the unit membrane bilayer apposed to the cytoplasm will be called the *inner leaflet* and the face apposed to the extracellular space, the *outer leaflet*.

RESULTS

A comparison of gap junctions observed in + EBUA and − EBUA retinas revealed expected differences in both the visibilities and patterns of staining of the junctions. Gap junction, synaptic and nonjunctional membranes in + EBUA retinas were of similar though not identical electron density [Fig. 1(a)], which rendered the search for gap junctions very difficult. When such junctions were found, such as the one between two large amacrine cell processes of sublayer 1 [Fig. 1(a)], they displayed the well-known septilaminar structure characterized by an intercellular gap of about 2 nm [Fig. 1(b,c)]. Alternatively, − EBUA material exhibited a dramatic difference in the electron density of the inner membrane leaflets of gap junctions when compared with other membranes. Thus gap junctions between large amacrine cell processes in sublayer 1 are easily detected at low magnifications [Fig. 2(a)]. A further salutary effect is the enhanced cytoplasmic differentiation obtained by avoiding the extraction inherent in acidic *en bloc* staining. A minor disadvantage is that the outer membrane leaflet appears perforated and does not stain confluently [Fig. 2(b)], thus preventing direct measurement of the extracellular gap. Even so, the gap junctions remain distinctive in that a characteristic ladder-like or periodic granulated zone fills the space between the inner membrane leaflets and the gap between the leaflets may be precisely measured for comparison with other images. Gap junctions were thus identified by (1) the significant electron density of their membranes; (2) the uniform reduction in the apparent space between membranes; (3) the presence of striations, granules or bridge-like extensions in the gap; and (4) the association of abundant electron-dense floccular material along the cytoplasmic face of the inner leaflet of the membrane.

The most objective measure of the presumed identity of gap junctional complexes in + EBUA and − EBUA material is obtained by the superposition of the transmission profiles from electron micrograph negatives. Figure 3 displays two such profiles whose absolute scaling demonstrates an identical separation of the inner leaflets of the membrane for the two staining protocols. The electron lucent gap in + EBUA material, as measured by the half-depth of the center trough between the outer membrane leaflets, was 1.97 nm (scan resolution = 23 nm traverse/100 sample points, or 0.2 nm; electron microscope resolution about 0.4 nm). This is an excellent match to the oft quoted 2 nm gap width. The center-to-center spacing of the inner membrane leaflets was 13.0 nm for both + EBUA and − EBUA retinas, which corresponds well to values of 14 nm for a total width of gap junctions between dogfish bipolar cells (Witkovsky and Stell, 1973) and 13 nm for the spacing between inner leaflets of gap junctions between turtle horizontal cells (Witkovsky, Owen and Woodworth, 1983). With this correlation established, we have classified these membrane specializations in − EBUA retinas as gap junctions.

The observations reported here involve the unequivocal identification of over a hundred

gap junctions in the goldfish IPL, 63 of which were of sufficiently good definition to characterize according to participating cell types. Unless the plane of section through a gap junction is nearly perpendicular to the plane of the membrane, it is very difficult to distinguish it from other membrane specializations. Thus the actual incidence of gap junctions is likely to be considerably greater than we have found. The sublayer of occurrence was recorded for 53 gap junctions and these are reported in Table 1. Of the total 63 junctions, 31 involved presumed homologous amacrine cell-amacrine cell pairings, 27 involved bipolar cell-bipolar cell pairings and 5 involved distinct amacrine cell-amacrine cell junctions with sufficient size or density differences in the appearances of the profiles to render them poor candidates for homologous junctions. However, we did not identify any gap junctions between profiles that we could confidently assign to different cell types. It is important to realize that our data are simply records of our observations and are not unbiased samples intended to represent actual distributions. Most of our examination centered on the distal IPL because the largest and most distinctive junctions seemed to be easier to find there.

Table 1.

	Sublayer					
	1	2	3	4	5	Total
AA	15	9	3	2	2	31
AAX	3	0	0	2	0	5
BB	9	4	1	0	3	17
Total	27	13	4	4	5	53

AA: gap junctions between similar amacrine cells.
AAX: gap junctions between dissimilar amacrine cells.
BB: gap junctions between bipolar cells.

Junctions between amacrine cell processes were particularly evident in the case of large caliber dendrites (diameters greater than 2 μm) coursing through sublayer 1 of the IPL (Figs 1 and 2). The processes were pale, contained loose aggregates of microtubules, with occasional elongate mitochondria, and the gap junctions were extensive, some exceeding 3 μm in length. Based on limited reconstructions from serial sections of two cells and observations of semi-serial sections of three other examples of very large diameter dendrites, we infer that each dendrite of these amacrine cells makes numerous homologous junctions. The junctional contacts between two processes in sublayer 1 of the IPL (Fig. 2) were followed in 6 serial sections. The profiles were traced, their contacts marked, and the superimposed profiles summarized in a single drawing (Fig. 4). Two large junctional patches were observed, separated by 5 μm (Figs 2 and 4). The large coupled dendrites were generally free of any protuberances or spines and their synaptic contacts were made onto other cells from virtually any location along

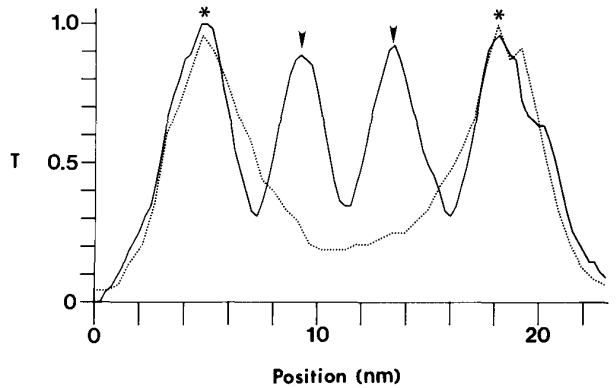

Fig. 3. Scanning microphotometry transmission curves for +EBUA (solid line) and −EBUA (dotted line) gap junctions of Fig. 1 and 2; transmission (T) of the negative as a function of true position in nanometers (nm). Each gap junction was scanned in a direction normal to the plane of the membrane (20 μm steps, 10 μm slit for +EBUA; 10 μm steps, 5 μm slit for −EBUA), and the total traverse length divided by the negative magnification to determine the scaling factor. Thus the images were scaled independently of each other, their peak transmissions normalized to 1.0 and superimposed. The inner membrane leaflets are marked by asterisks and are separated by 13.0 nm for both +EBUA and −EBUA gap junctions. The outer membrane leaflets appear only in +EBUA material and are indicated by arrowheads. The trough between the arrowheads, which corresponds to the electron-lucent line between the membranes in Fig. 1(c), has a half-width of 1.97 nm.

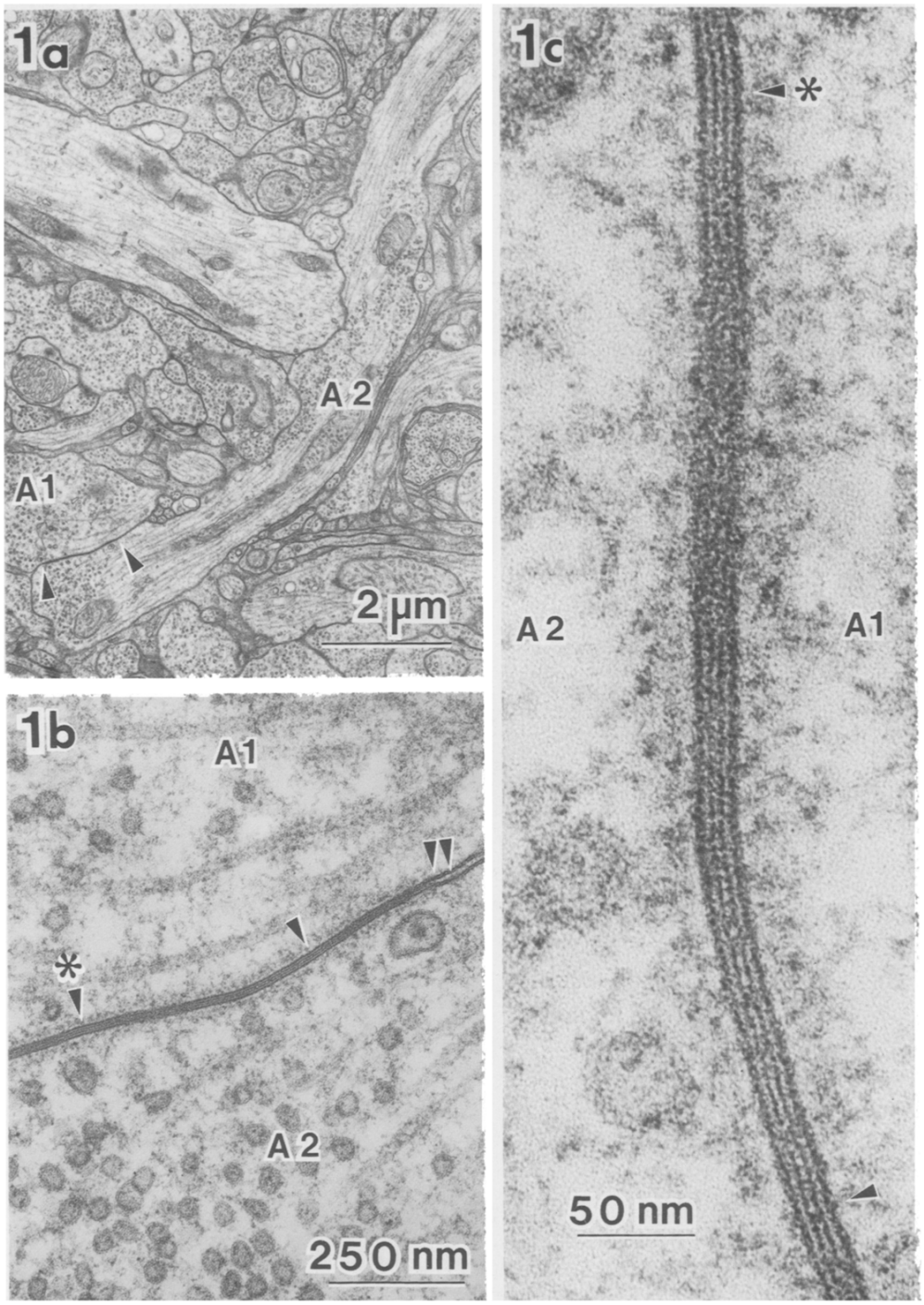

Fig. 1. A gap junction between large amacrine cell processes in sublayer 1 of the IPL; +EBUA retina. (a) Low magnification electron micrograph of a contact between two large caliber amacrine cell dendrites (A1, A2) which form a large gap junction as indicated by the arrowheads. Notice the relatively uniform membrane density and the lack of variation in electron density of most profiles throughout the preparation. (b) Higher power electron micrograph of the same gap junction indicated in 1a. The transition between nonjunctional membranes and the gap junction is indicated by the double arrowhead and particularly well-oriented regions are marked by single arrowheads. The asterisk is a reference point. (c) High power electron micrograph of the gap junction in 1b rotated clockwise 90°, revealing its definitive heptalaminar structure. Other distinctive features include a 2 nm intercellular gap, greater thickness of the inner as opposed to the outer membrane leaflets, and floccular accumulations along the cytoplasmic surfaces of the inner leaflets. The single arrowheads indicate exactly the same loci as in panel (b).

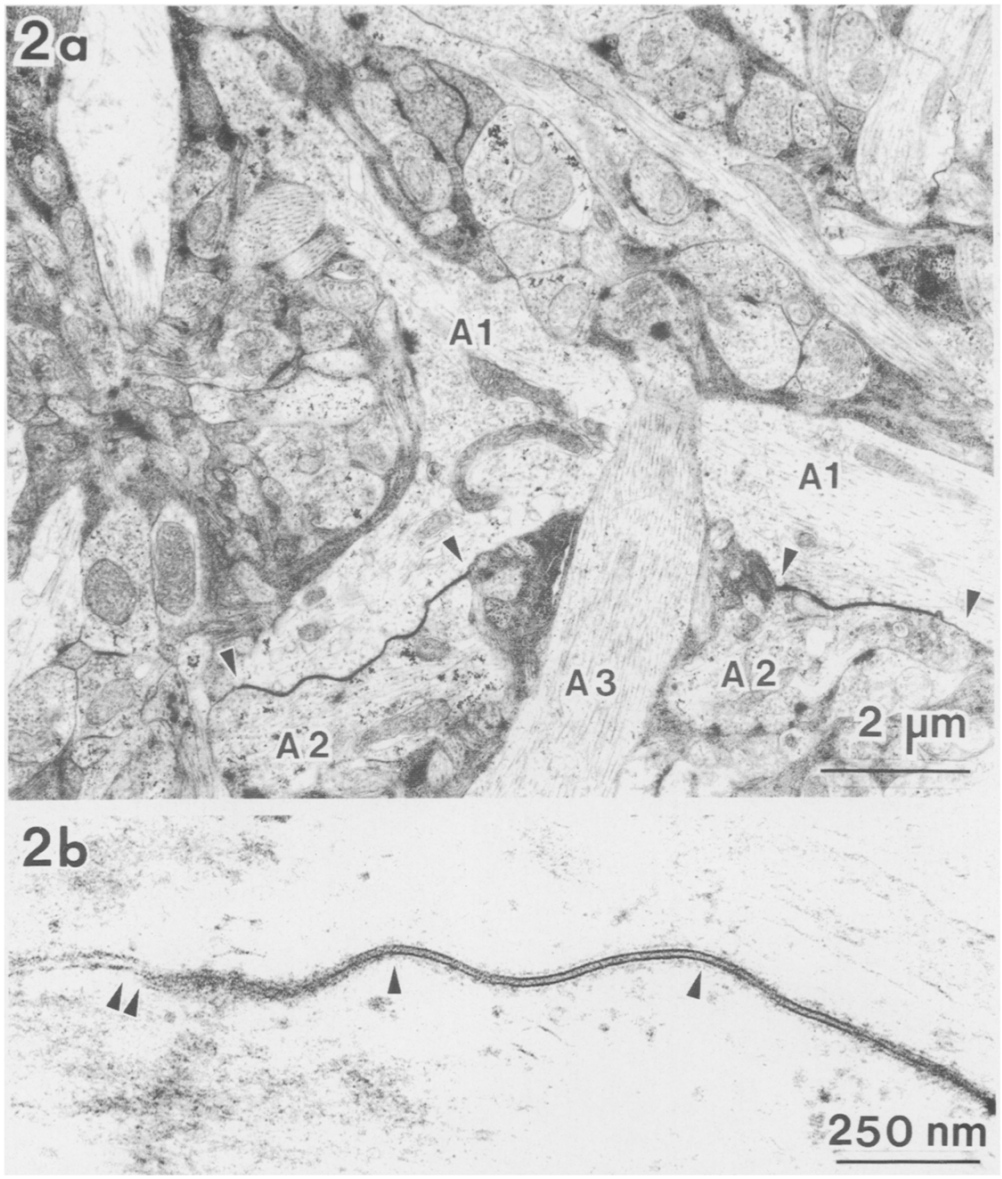

Fig. 2. Gap junctions between large amacrine cell processes in sublayer 1 of the IPL; −EBUA retina. (a) Low magnification electron micrograph of an intersection involving three large caliber amacrine cell dendrites (A1, A2, A3). Dendrites A1 and A2 form two extensive gap junctions as indicated by the arrowheads. Process A3 passes through the confluence, roughly normal to the trajectories of A1 and A2. Note the extreme difference between the electron densities of the gap junctions and all other membranes, as well as marked variations among the cytoplasmic compositions and electron densities of various profiles. (b) Higher power electron micrograph of a gap junction between two large caliber amacrine cell dendrites. The junction begins at the double arrowhead and the two single arrowheads indicate a region of particularly well-oriented membrane. Note the extremely dense inner membrane leaflets of the participating cells, the granular interior of the gap and the association of floccular material on the cytoplasmic faces of the membranes. The gap between the extracellular faces of the inner leaflets was 13.0 nm for this junction. This is a characteristic gap junction as viewed in material not stained *en bloc* with uranyl acetate.

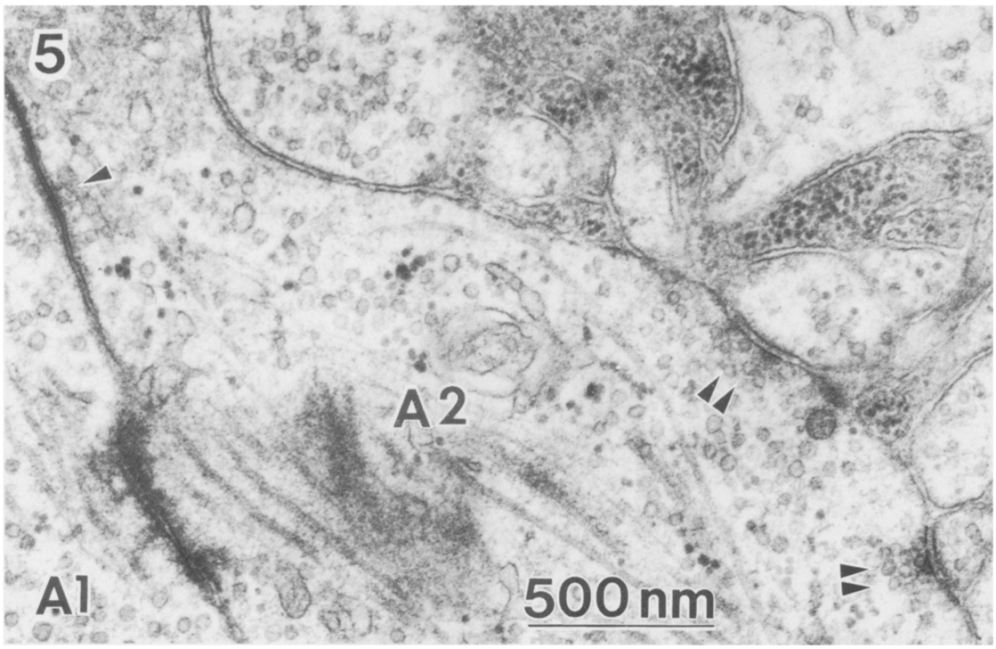

Fig. 5. Synaptic contacts of a coupled large caliber dendrite (A2) from Fig. 2. Dendrite A2 [Fig. 2(a), 4] forms two conventional synapses (double arrowheads) 1.75 μm away from the site of the gap junction (single arrowhead) between dendrites A1 and A2.

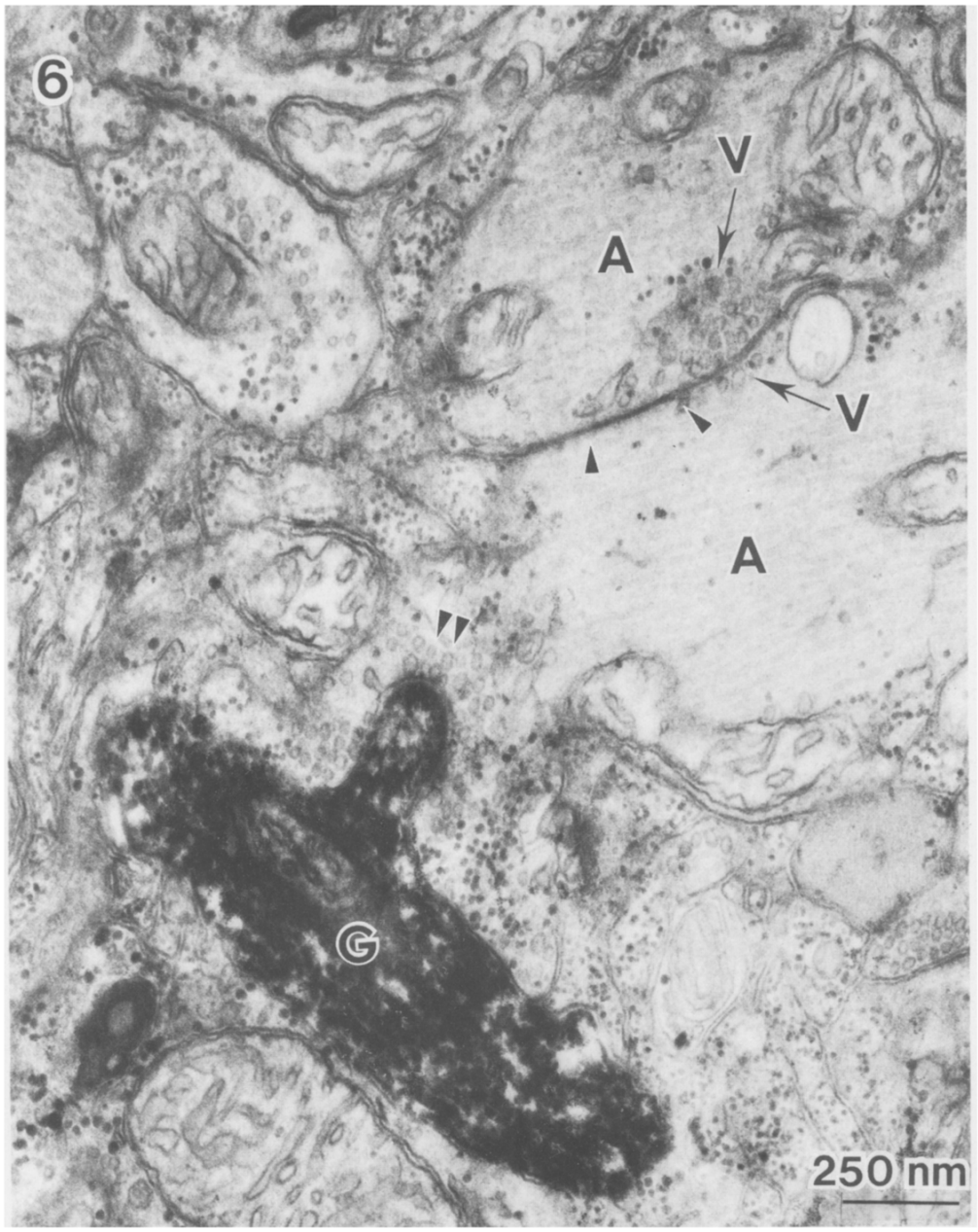

Fig. 6. A gap junction (pair of single arrowheads) between similar large caliber amacrine cell dendrites (A), one of which is pre-synaptic (double arrowhead) to a dendritic process from a ganglion cell (G) filled with HRP-catalyzed diaminobenzidine reaction product. Near the gap junction are bilateral aggregates of pleomorphic vesicles (V).

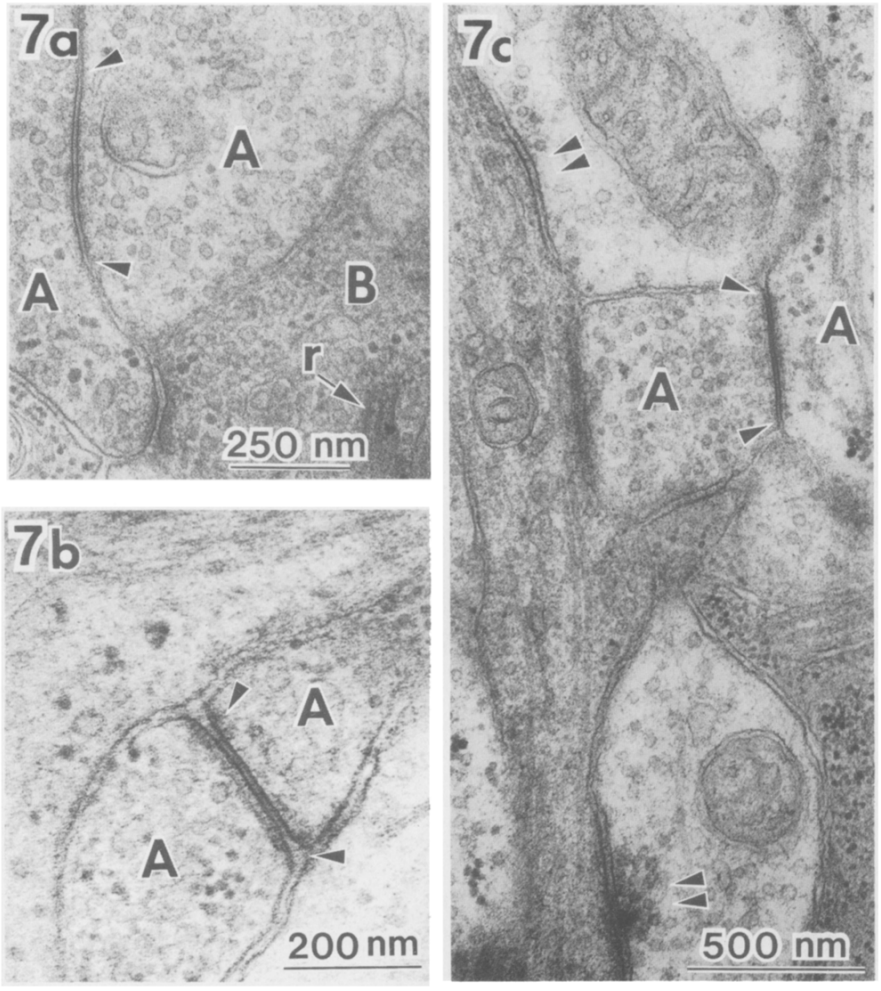

Fig. 7. Gap junctions (single arrowheads) between miscellaneous amacrine cell dendrites (A). (a) Gap junction between two moderate sized amacrine cell terminal swellings located in sublayer 2 of the IPL. One amacrine cell forms a junctional contact with a nearby bipolar cell (B); r, synaptic ribbon. (b) A gap junction between two small spine-like amacrine cell processes. The full extent of the junctional contact is less than 200 nm. (c) A gap junction between rather dissimilar amacrine cell dendrites in sublayer 1 of the IPL. One dendrite has a squarish, vesicle filled profile; the partner dendrite derives from a long, varicose process (not shown) unevenly filled with microtubules, glycogen granule clusters and synaptic vesicles. Two nearby profiles make conventional synaptic contacts (double arrowheads).

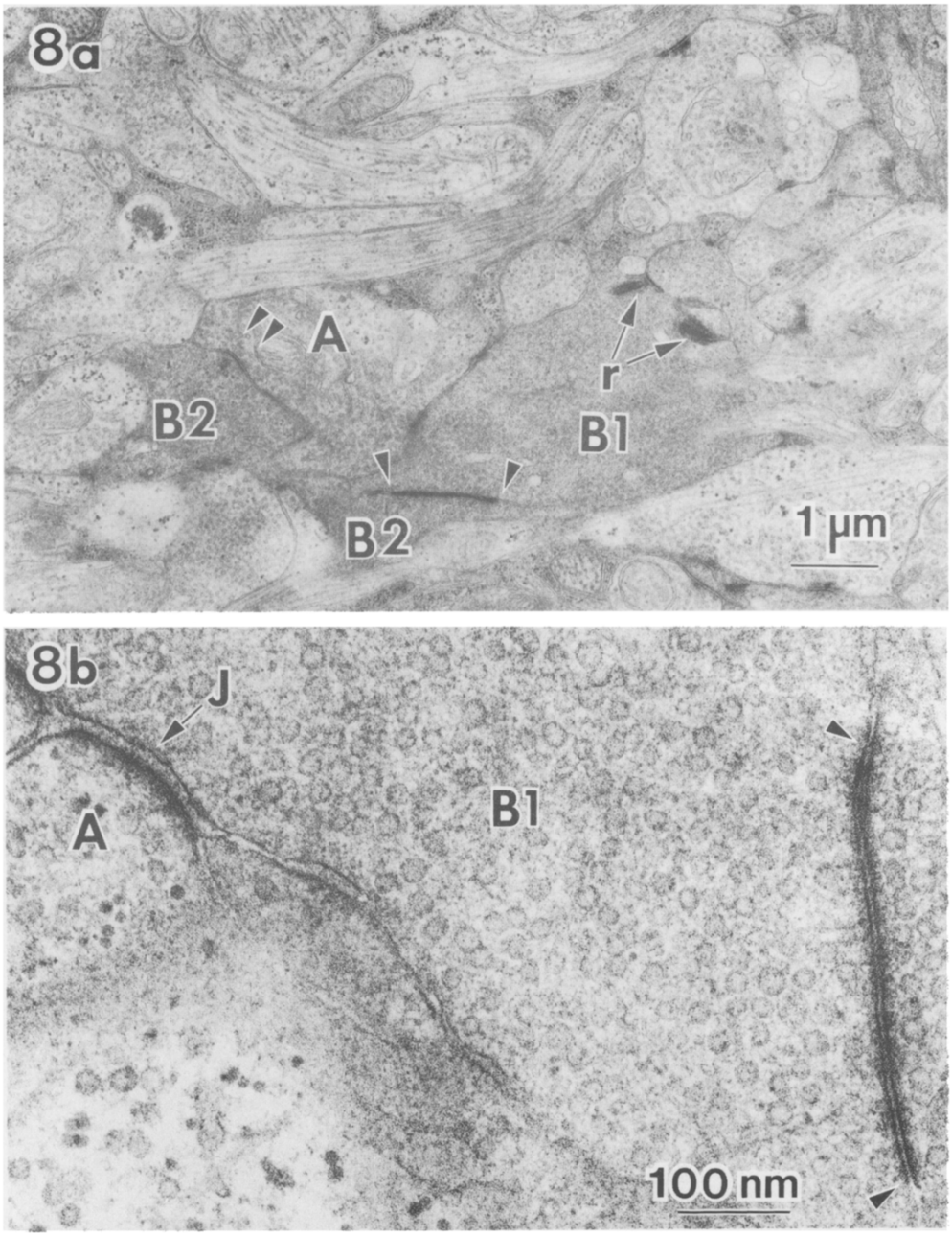

Fig. 8. Gap junction (single arrowheads) between bipolar cell synaptic terminals in sublayer 1 of the IPL. (a) Low magnification view of two bipolar cell terminals (B1, B2) with a gap junction between part of B1 and an irregularly shaped telodendron deriving from B2. B2 receives amacrine cell (A) input at the double arrowhead; r, bipolar cell ribbons. (b) Higher magnification view of a serial section to the junctional region, rotated 90 deg counter-clockwise. Bipolar cell gap junctions characteristically possess an abundance of electron-dense floccular material near the cytoplasmic face of the inner leaflet. A junctional complex (J) commonly found between bipolar cells and amacrine cells (A) is indicated for comparison of membrane spacing.

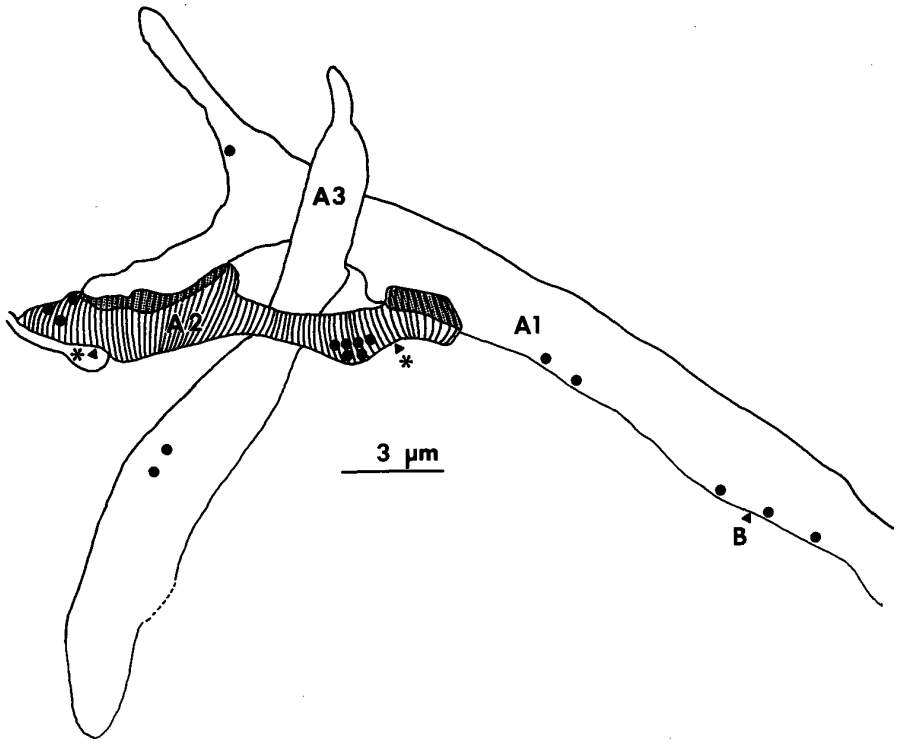

Fig. 4. A superposition drawing of the membrane contacts of large caliber amacrine cell dendrites. Profiles from six serial sections were aligned by eye and a composite illustration constructed of the size and placement of junctional membrane, synapses and the interleaving of three amacrine cell processes [A1, A2 and A3 from Fig. 2(a)]. Dendrite A2 (striated process) contacted dendrite A1 at two large patches (stippled regions), one 2.8 μm and the other 4.7 μm in length. Dendrite A1 formed six conventional synapses onto other amacrine cells or unidentified profiles (solid dots) and received one bipolar cell synapse (B). Dendrite A2 formed nine conventional synapses and received two conventional synapses (asterisks). Process A3 contracted neither A1 nor A2 and formed two conventional synapses.

their lengths (Fig. 5). Thus one could not specify the loci of probable contacts based upon varicosities, branching or other attributes likely to be visible at the light microscopic level. Synapses made by these processes onto other amacrine cells were typically mildly invaginated (Fig. 5). Altogether the two reconstructed processes made fifteen conventional pre-synaptic specializations onto other amacrine cells and unidentified processes (Fig. 4) and received input from amacrine cells and one bipolar cell. In a preparation designed to investigate the synaptology of individual retinal ganglion cells (Muller and Marc, 1985), we were fortunate to encounter synaptic input onto a ganglion cell dendritic spine from a large amacrine cell process engaged in a gap junction with a process of similar morphology (Fig. 6). Thus these particular amacrine cells seem to be part of a feed-forward system from bipolar cells → coupled amacrine cell network → ganglion cells.

Many pairs of smaller processes and synaptic terminal swellings were observed to be coupled (Fig. 7). In most instances the profiles seemed to arise from similar classes of amacrine cells, most often pale, vesicle-filled terminals. The sizes of the junctions were quite variable, between 200 nm and 1 μm, although they were always much smaller than those between the large diameter dendrites previously described. Of course it is possible that some of the apparently smaller junctions were the irregular edges of large gap junctions. Smaller gap junctions could easily have escaped our notice. Some junctions were close to sites of synaptic contact and others were between small spine-like protruberances [Fig. 7(b)]. A few instances involved junctions between profiles that were rather dissimilar in terms of size, cytoplasmic density, microtubule content or glycogen content [e.g. Fig. 7(c)], so they were not classified as homologous junctions. It should be acknowledged, however, that

variations in cytoplasmic electron density, inclusions, etc. occur within a single process so that individual samples of that process might lead one to erroneously conclude that those samples were derived from different entities. Thus we stress that we have merely identified these cases as dissimilar and not definitively heterologous.

Finally, junctions were found between processes arising from bipolar cell terminals (Fig. 8). Bipolar cell gap junctions were particularly easy to recognize at low magnifications due to their accretions of very electron dense material along the cytoplasmic faces of the inner membrane leaflets. Most often we identified contacts between moderately electron dense, slender processes that were filled with vesicles and only in a few cases were we able to trace the profiles back to bipolar cell terminals containing synaptic ribbons. As an additional observation, however, the identification of bipolar cell profiles is quite reliable in −EBUA retinas as they have very distinctive electron-dense cytoplasm filled with synaptic vesicles [e.g. Fig. 8(a)]. All bipolar cell types exhibit this virtually diagnostic attribute. In contrast, +EBUA retinas display little difference in electron density between bipolar cells and all other cell types. The lengths of the gap junctions were difficult to assess as they most often involved irregularly shaped telodendria of bipolar cells. Small focal contacts were observed as well as long regions of apposition approaching 0.5 μm in length. Gap junctions between bipolar cells were found in both proximal and distal IPL, and involved telodendria arising from large terminals. For example, process B1 in Fig. 8(a) is a relatively large terminal swelling in sublayer 1 of the IPL. Its size is appropriate for that of a type *a* mixed rod-cone bipolar cell (see Ishida *et al.*, 1980), although it is possible that cone bipolar cells also engage in gap junctions. A neighboring bipolar cell terminal (B2) is represented by but a part of its terminal swelling and gives rise to a very irregular extension which contacts B1, forming a good length of gap junctional contact. Seen at higher magnification in a semiserial section [Fig. 8(b)], the gap junction is seen to be heavily decorated on its cytoplasmic surfaces with an extremely electron dense material. This is characteristic of gap junctions between bipolar cell terminals and is a variable attribute of gap junctions between amacrine cells.

DISCUSSION

The differential staining attributes of retinal gap junctions with and without *en bloc* uranyl acetate exposure have been previously described by Witkovsky and Stell (1973) for dogfish retina. Our findings are virtually identical and provide an objective basis for the spacing match of the inner leaflets of the junctional membranes. The additional beneficial feature of the −EBUA protocol is an enhanced contrast between gap junctional and other unit membranes. This allows surveys of tissue at low magnification for possible well-oriented gap junctions. We stress that our numerical observations merely show that gap junctions can be observed at every level of the IPL. In fact, knowing the laminar distribution of gap junctions is not intrinsically useful for circuitry analysis. The appropriate focus from this juncture should be the characterization of the specific kinds of amacrine and bipolar cells engaging in gap junctions, which will lead to an appropriately precise description of gap junction distribution.

We have found the IPL of the goldfish retina to contain gap junctions qualitatively similar to those described for catfish amacrine cells (Naka and Christensen, 1981) and dragonet bipolar cells (Van Haesendonck and Missotten, 1983b). Thus the goldfish seems to possess the same attributes of cell coupling in the IPL as rather disparate orders of teleostean fish. The coupled amacrine cells described in catfish retina (Naka and Christensen, 1981) are transient amacrine cells which are similar in gross morphology to transient amacrine cells identified by Procion Yellow dye injection in carp (Murakami and Shimoda, 1975; Famiglietti *et al.*, 1977) and those shown to be dye-coupled by Lucifer Yellow injections (Teranishi *et al.*, 1984); such cells possess large prolate somas and a few large diameter proximal dendrites which extend laterally and course obliquely into the IPL to form two strata. Dye coupling among transient amacrine cells has also been reported in turtle retina (Jensen and Devoe, 1982). The large, coupled amacrine cell processes we observe are consistent with the expectation that the goldfish retina should contain coupled transient amacrine cells. One striking characteristic of these cells is the apparent dearth of spines, protuberances, varicosities or other surface specializations of the dendrites at synaptic sites (at least within the large diameter regions) that would serve as indices of contact loci at the light microscope level. The sole attribute of synaptic output is a variable invagination of otherwise smooth, sim-

ple processes, and the targets are the dendrites of certain amacrine and ganglion cells.

The gap junctions between these dendrites are extensive, perhaps several square microns in area, similar to those between fish horizontal cells and between horizontal cell axon terminals (Yamada and Ishikawa, 1965; Witkovsky and Dowling, 1969; Witkovsky and Stell, 1973; Marc *et al.*, 1978). There are several intriguing similarities between these particular coupled dendrites and horizontal cell axon terminals: (1) both are large diameter cable-like elements; (2) both are richly endowed with microtubules running parallel to the long axis of the process, although those of the horizontal cell axon terminals are much more orderly; (3) mitochondria are sparsely distributed in the processes; (4) their output synapses are moderate in size and are made directly from the large diameter profiles without significant structural specialization such as spines or varicosities [Marc and Liu, 1984; Sakai and Naka, 1985; Fig. 3(a)]; and (5) both form multiple patches of gap junctions. If the amacrine cell dendrites possess gap junctions with a frequency and size distribution similar to horizontal cell axon terminals, extensive electrical coupling is likely (e.g. Witkovsky *et al.*, 1983). One very important caveat is that certain types of ganglion cells in the catfish retina have been observed to possess some pre-synaptic specializations (Sakai *et al.*, 1986) and we have no simple means to exclude the possibility that some of the gap junctions observed here involve ganglion cell coupling.

The medium sized and small amacrine cell terminals and processes that we observed to be coupled seem to arise from different varieties of cells than the large amacrine cell dendrites. Some of the processes appear lobular, with a small diameter pre-terminal dendrite expanding into a rounded or lobed terminal, as observed in glycineric (Marc and Lam, 1981) or GABAergic (Marc *et al.*, 1978) amacrine cells, or varicose, with ovoid swellings occurring along a thin dendrite, as exhibited by indole-accumulating amacrine cells (Holmgren-Taylor, 1983a, b; Marc *et al.* 1987 and in preparation). Teranishi, Negishi and Kato (1984) have recently reported that some On-sustained amacrine cells exhibit dye coupling and some of the inter-amacrine cell junctions observed here were found in the most proximal regions of the IPL, where the On-sustained GABAergic amacrine cells of the goldfish retina are believed to arborize (Marc *et al.*, 1978). By applying oblique section analysis to EM-autoradiography of amacrine cells labeled by [3H] neurotransmitter uptake, we should be able to further evaluate the identities of these coupled amacrine cell processes.

Gap junctions between ectotherm bipolar cell terminals were first reported in the retina of the smooth dogfish (Witkovsky and Stell, 1973), and appeared to involve junctions between bipolar cells of the same variety. The components of a bipolar cell that could bear gap junctions are: (1) the single axon that descends from the bipolar cell soma into the IPL; (2) varicose swellings that occur along the axon (pure cone bipolar cells; Scholes, 1975) or the single terminal swelling at the end of the axon (mixed rod-cone bipolar cells; Scholes, 1975; Ishida *et al.*, 1980); or short, irregular finger-like processes known as telodendria that extend from terminal swellings (Ishida *et al.*, 1980). Initially, gap junctions between goldfish bipolar cells were difficult to document because the junctions were located on the telodendria in most cases. Once we learned the cytological features of bipolar cell axon terminals and their telodendria, however, we could readily identify instances of coupling between bipolar cell telodendria. This is slightly different from the dragonet retina (Van Haesendonck and Missotten, 1983a) where the frequency of bipolar cells is extremely high in the dorsal pure cone region. Thus the bipolar cell terminals form grid-like arrays in the IPL with neighboring terminals so close as to allow direct contact (Van Haesendonck and Missotten, 1983a, b). Furthermore, their telodendria are short, lying in excellent alignment with the parent terminals. Van Haesendonck and Missotten (1983b) pointed out that different kinds of bipolar cells were engaged in gap junctions in the dragonet, hence these junctions may in fact be physiologically heterologous. This is a complexity that we cannot resolve for the moment because the bipolar cell terminal density at any given level of the goldfish IPL appears to be so low (Marc, 1982) that there can be little or no direct contact between the large terminal swellings *per se*. However, mixed rod-cone bipolar cells in the goldfish and other cyprininds are known to possess filamentous extensions reminiscent of cone telodendria (Ishida *et al.*, 1980; Scholes, 1975). The functions of these processes are not known, but is now evident that they could at least serve as a means of mediating electrical coupling between bipolar cells. In general, the

presence of telodendria, the localization of bipolar cell gap junctions in both distal and proximal IPL, and the large sizes of the terminals involved (e.g. Fig. 8), all indicate that some of the bipolar cells participating in coupling are of the mixed rod-cone variety. Recently, Kujiraoka and Saito (1986) reported that both On-center and Off-center bipolar cells in the carp retina were electrically coupled and that some could be shown to be dye coupled. We suggest that a major mechanism for this coupling is at the level of the bipolar cell terminals. Some coupling could occur at the dendritic level, as Raviola and Gilula (1975) have suggested from electron microscopy of rabbit and monkey retina, but we have seen no evidence of dendritic coupling among goldfish bipolar cells. Not all kinds of bipolar cells are likely to be coupled at the terminal level. Considering that pure cone bipolar cells in the rudd (a cyprinid fish closely allied to the goldfish) possess varicose axons with no notable telodendria (Scholes, 1975) and that such cone bipolar cells are likely to be no more closely spaced that the mixed rod-cone varieties, homologous coupling at the terminal level would seem to be precluded because like pairs of cone bipolar cells would not come in contact. Heterologous coupling cannot be ruled out, however.

Heterologous coupling in the vertebrate IPL, as typified by gap junctions between AII amacrine cells and cone bipolar cells in the cat retina (Famiglietti and Kolb, 1975), seems to be rare or cryptic in the teleost retina. While such a phenomenon may yet be uncovered, teleosts and mammals lack a common substrate for this particular kind of heterologous coupling: rods and certain cones share the same bipolar cells in teleosts (Stell, 1967; Ishida *et al.*, 1980), whereas heterologous coupling between mammalian pure cone bipolar cells and AII amacrine cells presumably subserves the function of transfering pure rod bipolar cell signals to pathways having direct access to ganglion cells (Nelson and Kolb, 1983).

This leads us to a consideration of the terminology for expressing coupling relationships. It is difficult to characterize a gap junction representing homologous coupling in most anatomical preparations. Exceptions are rod-rod gap junctions in carp (Witkovsky, Shakib and Ripps, 1974) or those between pairs of H1 horizontal cells in goldfish (Marc *et al.*, 1978). Within the goldfish IPL, the gap junctions appear to represent homologous coupling but we have no grounds on which to assert that the coupling is physiologically homologous. For example, electrical coupling occurs between the same nominal physiological type of carp bipolar cells, but the cyprinid retina probably contains three species of On-center and two species of Off-center mixed rod-cone bipolar cells (Ishida *et al.*, 1980) and gap junctions are made between structurally different classes of bipolar cells in the dragonet retina that terminate at the same level of the IPL (Van Haesendonck and Missotten, 1983). Teleost cones further demonstrate the subtleties of analyzing coupling mediated by gap junctions. Teleost cone pedicles form gap junctions with each other (Witkovsky *et al.* 1974), which represents anatomically homologous coupling. However, Marchiafava (1985) has demonstrated that the individual red- and green-sensitive members of isolated double cones in the tench retina are apparently electrically coupled. The anatomical substrate for the physiological findings remains unknown, but telodendria of fish cones are known to make heterochromatic contacts (Stell, 1980). Though these cones are clearly recognizing other cones in selecting their contacts, their coupling is physiologically heterologous when spectral properties are considered. Such relationships may also exist in the IPL, although we lack the means to discriminate them at the moment. Our impression is that the majority of the gap junctions in the goldfish inner plexiform layer represent homologous coupling.

In summary, intercellular coupling via gap junctions is evident throughout the teleost inner plexiform layer. It is also clear why gap junctions have not been prominently reported in the cyprinid IPL despite previous surveys of synaptic relations (e.g. Witkovsky and Dowling, 1969; Holmgren-Taylor, 1983b): vertical sections contain a powerful quantitative bias against gap junctions in general and in favor of the more abundant conventional synapses in particular. The chance of finding gap junctions is improved by examining oblique or horizontal sections and employing staining tactics that increase the contrast between gap junctions and other unit membranes. Within the constraints previously discussed, it would appear that a great fraction of the coupling in the cyprinid IPL is homologous. As our comprehension of retinal organization now stands, there is coupling among sets of rods, cones, horizontal cells, bipolar cells and amacrine cells. The establishment of low resistance paths among members of

one type (subtype) of retinal cell leading to the intercellular spread of current and exchange of small molecules seems to be the rule rather than the exception in the retina.

Acknowledgements—This research was supported by NIH grant EY 02576. We thank Drs S. C. Massey and E. Van Haesendonck for discussions. We are also grateful to the reviewers for insightful criticisms which greatly improved the manuscript.

REFERENCES

Dowling J. E. (1979) Information processing by local circuits: The vertebrate retina as a model system. In *The Neurosciences, Fourth Study Program* (Edited by Schmitt F. O. and Worden F. G.), pp. 163–181. MIT Press, Cambridge, Mass.

Famiglietti E. V. Jr and Kolb H. (1975) A bistratified amacrine cell and synaptic circuitry in the inner plexiform layer of the retina. *Brain Res.* **84,** 293–300.

Famiglietti E. V. Jr, Kaneko A. and Tachibana M. (1977) Neuronal architecture of ON and OFF pathways to ganglion cells in carp retina. *Science, N.Y.* **198,** 1267–1269.

Hayat M. A. (1981) *Fixation for Electron Microscopy.* Academic Press, New York.

Holmgren-Taylor I. (1983a) Synaptic organization of the indoleamine accumulating neurons in the cyprinid retina. *Cell Tiss. Res.* **229,** 317–335.

Holmgren-Taylor I. (1983b) Synapses of the inner plexiform layer in the retina of cyprinid fish. *Cell Tiss. Res.* **229,** 337–350.

Ishida A. T., Stell W. K. and Lightfoot D. O. (1980) Rod and cone inputs to bipolar cells in the goldfish retina. *J. comp. Neurol.* **191,** 315–335.

Jenson R. J. and DeVoe R. D. (1982) Ganglion cells and (dye-coupled) amacrine cells in the turtle retina that have possible synaptic connection. *Brain Res.* **240,** 146–150.

Kolb H. and Nelson R. (1985) Functional neurocircuitry of amacrine cells in the cat retina. In *Neurocircuitry of the Retina, A Cajal Memorial* (Edited by Gallego A. and Gouras P.), pp. 215–232. Elsevier, New York.

Korte G. E. and J. Rosenbluth (1980) Freeze-fracture study of the post-synaptic membrane of the cerebellar mossy fiber synapse in the frog. *J. comp. Neurol.* **193,** 698–700.

Kujiraoka T. and Saito T. (1986) Electrical coupling between bipolar cells in carp retina. *Proc. natn. Acad. Sci. U.S.A.* **83,** 4063–4066.

Lowenstein W. R. (1975) Permeable Junctions. *Cold Spring Harb. Symp. quant. Biol.* **40,** 49–63.

Marc R. E. (1982) The spatial organization of neurochemically classified interneurons in the goldfish retina. I. Local patterns. *Vision Res.* **22,** 589–608.

Marc R. E. (1986) Neurochemical stratification in the inner plexiform layer of the vertebrate retina. *Vision Res.* **26,** 223–238.

Marc R. E. and Lam D. M. K. (1981) Glycinergic pathways in the goldfish retina. *J. Neurosci.* **1,** 152–165.

Marc R. E. and Liu W.-L. S. (1984) Horizontal cell synapses onto glycine-accumulating interplexiform cells. *Nature, Lond.* **311,** 266–269.

Marc R. E. and Liu W.-L. S. (1985) (3H) Glycine-accumulating neurons of the human retina. *J. comp. Neurol.* **232,** 241–260.

Marc R. E., Liu W.-L. S., Scholz K. and Muller J. F. (1987) Serotonergic amacrine cells of the goldfish retina. *Invest.Ophthal. visual Sci., Suppl.* **28,** 277.

Marc R. E., Stell W. K., Bok D. and Lam D. M. K. (1978) GABA-ergic pathways in the goldfish retina. *J. comp. Neurol.* **182,** 221–246.

Marchiafava P. L. (1985) Cell coupling in double cones of the fish retina. *Proc. R. Soc. B* **226,** 211–215.

Muller J. F. and Marc R. E. (1985) GABA-ergic and glycinergic synapses onto goldfish retinal ganglion cells. *Invest. Ophthal. visual Sci., Suppl.* **26,** 95.

Murakami M. and Shimoda Y. (1975) Identification of amacrine and ganglion cells in the carp retina. *J. Physiol., Lond.* **264,** 801–818.

Naka K.-I. and Christensen B. (1981) Direct electrical connections between transient amacrine cells in the catfish retina. *Science, N.Y.* **214,** 462–464.

Nelson R. and Kolb H. (1983) Synaptic patterns and response properties of bipolar and ganglion cells in the cat retina. *Vision Res.* **23,** 1183–1195.

Raviola E. and Gilula N. B. (1975) Intramembrane organization of specialized contacts in the outer plexiform layer of the retina. A freeze-fracture study in monkeys and rabbits. *J. Cell Biol.* **65,** 192–222.

Raviola E. and Raviola G. (1967) Light and electron microscopic observations on the inner plexiform layer of the rabbit retina. *Am. J. Anat.* **120,** 403–426.

Raviola E. and Raviola G. (1982) Structure of the synaptic membranes in the inner plexiform layer of the retina: A freeze-fracture study in monkeys and rabbits. *J. comp. Neurol.* **209,** 233–248.

Sakai H. and Naka K.-I. (1985) Novel pathway connecting the outer and inner vertebrate retina. *Nature, Lond.* **315,** 570–571.

Sakai H., Naka K.-I. and Dowling J. E. (1986) Ganglion cell dendrites are presynaptic in catfish retina. *Nature, Lond.* **319,** 495–497.

Scholes J. (1975) Colour receptors and their synaptic connexions in the retina of the cyprinid fish. *Phil. Trans. R. Soc. B* **270,** 61–118.

Stell W. K. (1967) The structure and relationships of horizontal cells and photoreceptor-bipolar synaptic complexes in the goldfish retina. *Am. J. Anat.* **121,** 401–424.

Stell W. K. (1980) Photoreceptor-specific synaptic pathways in goldfish retina: a world of colour, a wealth of connections. In *Colour Vision Deficiencies V* (Edited by Verriest G.), pp. 1–14. Adam Hilger, London.

Teranishi R., Negishi K. and Kato S. (1984) Dye coupling between amacrine cells in carp retina. *Neurosci. Lett.* **51,** 73–78.

Van Haesendonck E. and Missotten L. (1983a) Stratification and square pattern arrangements in the dorsal inner plexiform layer in the retina of *Callionymus lyra L. J. Ultrastruct. Res.* **83,** 296–302.

Van Haesendonck E. and Missotten L. (1983b) Interbipolar contacts in the dorsal inner plexiform layer in the retina of *Callionymus lyra L. J. Ultrastruct. Res.* **83,** 303–311.

Witkovsky P. and Dowling J. E. (1969) Synaptic relationships in the plexiform layers of the carp retina. *Z. Zellforsch.* **100,** 60–82.

Witkovsky P. and Stell W. K. (1973) Retinal structure in the smooth dogfish *Mustelus canis*: Electron microscopy of serially sectioned bipolar cell synaptic terminals. *J. comp. Neurol.* **150,** 147–168.

Witkovsky P., Owen W. G. and Woodworth M. (1983) Gap junctions along the perikarya, dendrites and axon terminals of the luminosity-type horizontal cell of the turtle retina. *J. comp. Neurol.* **216,** 359–368.

Witkovsky P., Shakib M. and Ripps H. (1974) Interreceptoral junctions in the teleost retina. *Invest. Ophthal.* **13,** 996–1009.

Yamada E. and Ishikawa T. (1965) The fine structure of the horizontal cells in some vertebrate retinae. *Cold Spring Harb. Symp. quant. Biol.* **30,** 383–392.

Zimmerman R. P. (1983) Bar synapses and gap junctions in the inner plexiform layer: Synaptic relationships of the interstitial amacrine cell of the retina of the cichlid fish, *Astronotus ocellatus*. *J. comp. Neurol.* **218,** 471–479.